Supramolecular DNA photonic hydrogels for on demand control of coloration with high spatial and temporal resolution

*Yixiao Dong, J. Dale Combs, Cong Cao, Eric R. Weeks, Alisina Bazrafshan, SK Aysha Rashid, Khalid Salaita**

Address: Y. Dong, J. Dale Combs, A. Bazrafshan, SK A. Rashid, K. Salaita

Department of Chemistry, Emory University, 1515 Dickey Drive, Atlanta, Georgia, 30322, USA

C.Cao, E. R. Weeks

Department of Physics, Emory University, 400 Dowman Drive, Atlanta, Georgia, 30322, USA

*Corresponding author: k.salaita@emory.edu

Keywords: DNA supramolecular hydrogel, photonic crystals, on-demand assembly, high resolution laser patterning, chromatic response

Abstract

Hydrogels embedded with periodic arrays of nanoparticles display striking photonic crystal coloration that may be useful for applications such as camouflage, anti-counterfeiting, and chemical sensing. Dynamically generating color patterns requires control of nanoparticle organization within a polymer network on-demand which is challenging. We solve this problem by creating a DNA hydrogel system that shows a 50,000-fold decrease in modulus upon heating by ~10 °C. Magnetic nanoparticles entrapped within these DNA gels generate structural color only when the gel is heated and a magnetic field is applied. Spatially controlled photonic crystal coloration was achieved by photopatterning with near-infrared illumination. Color was "erased" by illuminating or heating the gel in the absence of an external magnetic field. The on-demand assembly technology demonstrated here may be beneficial for developing a new smart materials with potential applications in erasable lithography, encryption, and sensing.

Introduction

Photonic crystals (PCs) are periodic arrays of nano- and micro-scale materials that can display striking colors due to Bragg diffraction[1]. In contrast to dyes and pigments which absorb specific wavelengths of light, PCs are resistant to photobleaching and their color is dependent on the spatial periodicity of the material rather than its chemical composition. Indeed, as predicted by Bragg's law of diffraction, the specific coloration of PCs can be tuned by adjusting the spacing in the periodic array.

The ability to create responsive PC materials that can generate coloration in space and time is highly desirable as such materials have important applications in sensing[19-21], camouflage[5], and anti-counterfeiting inscriptions.[22] [23-28] Most responsive PC materials are generated by embedding or etching PC structures in a hydrogel matrix that displays a volume change (ie. swelling or collapse) in response to specific types of input[28]. These changes in the matrix will in turn modulate the lattice constant of the PC and hence tune the color of the material. One of the greatest challenges in this area is on-demand patterning of the nanoparticle re-organization, as the PC nanoparticles are physically confined within the matrix of the hydrogel. In other words, the challenge pertains to creating periodic assemblies of nanoparticles within a hydrogel from a disordered array with spatial and temporal control. Herein, we address this challenge and create a PC hydrogel that displays on-demand coloration by using DNA supramolecular hydrogels that can rapidly and locally switch between crosslinked and de-crosslinked states using an opto-thermal trigger.

To achieve on demand assembly with high spatial and temporal resolution two conditions must be met: 1) A hydrogel must undergo local, reversible, and transient de-crosslinking upon

specific inputs, and 2) Nanoparticles should rapidly translocate and organize within the hydrogel during transient de-crosslinking. To the best of our knowledge, there are no reported examples of nanocomposite hydrogels that meet these conditions. The most commonly adopted approach to form PC hydrogels requires first organizing the PC material using an external magnetic, gravitational, or electric field. Once organized, the hydrogel is crosslinked in a way that the nanoscale periodicity is locked and preserved after the removal of external field.[29-30] This is due to the large energy barrier to diffusion created by the hydrogel network which prevents nanoparticle mobility inside the hydrogel.

Our approach is illustrated in **Figure 1** where we used a DNA supramolecular hydrogel[33] constructed from palindromic single stranded DNA (ssDNA) with three self-complementary domains (red, green, and blue domains in **Figure 1a**). To create the PC, we used superparamagnetic magnetite nanoparticles (MNPs) coated with poly(ethylene glycol) (PEG) that assemble into periodic structures under an external magnetic field (**Figure 1b,** also see **Figure S1** showing TEM images of different sizes of MNPs**)**. PEGylated MNPs are stable enough to assemble in aqueous buffers with higher ionic strength which is necessary for DNA hydrogel formation (**Figure S2**). Given that crosslinks are exclusively created using hybridized DNA strands, denaturing the DNA allows complete de-crosslinking of the hydrogel and thus lifting the energy barrier for particle mobility (**Figure 1c)**. In contrast to other supramolecular hydrogels, pure DNA-based hydrogels in this work display faster gelation kinetics with time resolution of seconds and a relative rigid network that can hold the in-situ assembled structure. These two features are advantageous for on demand structural coloration and de-coloration.

The key design criteria for creating an on-demand PC material are illustrated using a simplified energy diagram in **Figure 1c**, where the y-axis represents the free energy of the system and the x-axis represents an order parameter (e.g. the particle organization). State 1 illustrates an initial condition where particles are randomly distributed inside the hydrogel network, while state 2 represents ordered particles that form the PC. Under the influence of an external magnetic field (B), state 1 is higher in energy compared to state 2 due to the potential energy of the magnetic dipole moments of the MNPs. In order for the particles to organize, they must overcome the energy barrier required for movement across the DNA hydrogel network. This barrier is large when the DNA is fully hybridized (black curve **Figure 1c**) and hence particles are locked in place. When the DNA is denatured, the barrier reaching state 2 is lowered and thus allowing for translocation to occur (red curve, **Figure 1c**). **Figure 1d** illustrates the overall cycle of triggered on-demand assembly (patterning) and disassembly (erasing) of the PC within the DNA hydrogel. In our case, we trigger DNA disassembly using the broad absorption spectrum and high photothermal conversion efficiency of MNPs. This can locally and transiently melt the DNA network and dramatically lower the particle translocation energy barrier (**Figure S3**). The simulation of photo-thermal effect of the laser on the hydrogel is illustrated in **Figure S4**, which proves the heat generated by MNPs are large enough to dehybridize the surrounding DNA duplex networks. Upon illumination, the MNPs should generate heat and locally melt the gel as they translocate and align with an external magnetic field, therefore forming a periodic PC structure. Upon removal of illumination, rapid heat dissipation should result in re-hybridization of DNA strands. This locks the patterned PC

in the DNA gel. Notably, these PC patterns can be rapidly “erased” by illumination in the absence of an external magnetic field.

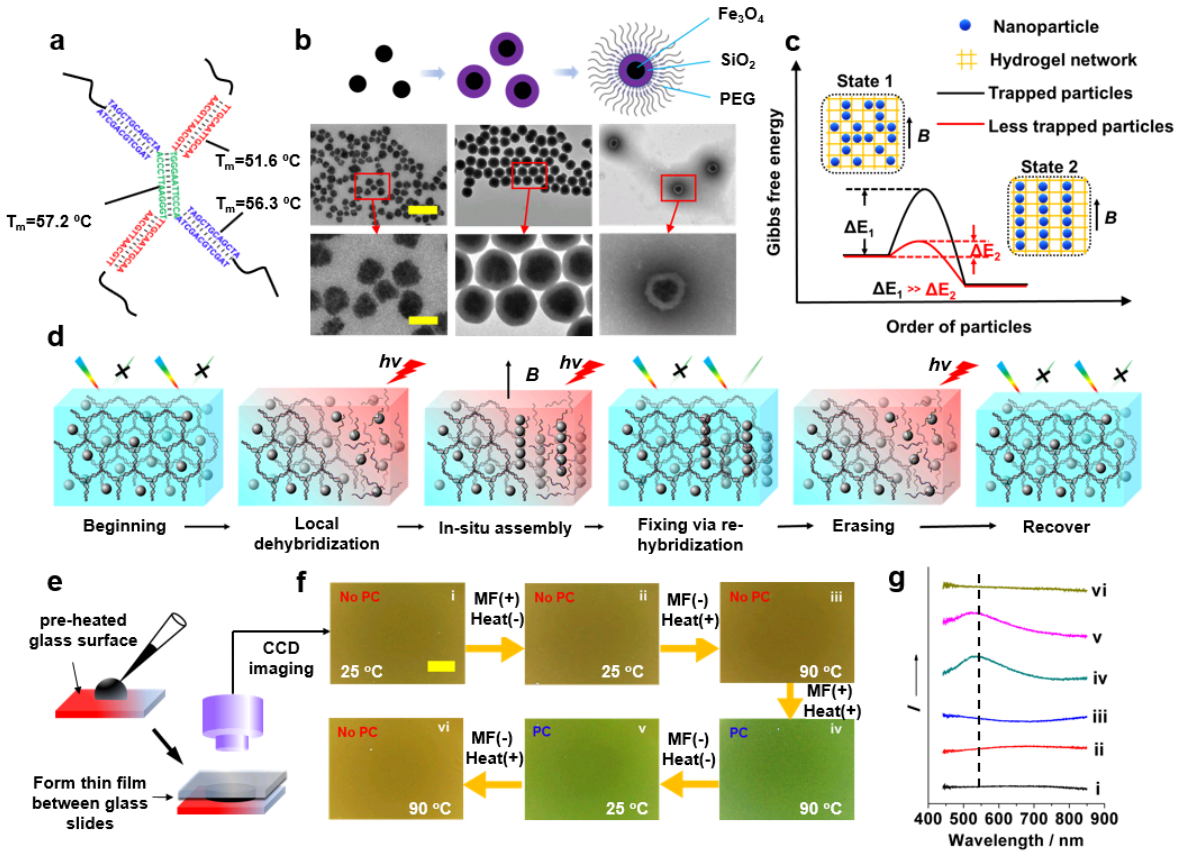

Figure 1. Design and testing of the DNA hydrogel system for on demand patterning and erasing. a) Design of a purely DNA supramolecular hydrogel system in which the DNA hydrogel is formed from three different palindromic sequence domains located on a single strand. b) Schematic of MNP synthesis and corresponding TEM images of real samples. Magnetite nanoparticles (~120 nm) are coated with a silica shell (~30 nm) first and then a layer of PEG. (scale bar: 500 nm for upper set and 125 nm for lower set) c) Theoretical energy diagram of in-situ assembly of the hydrogel. d) Mechanism of in-situ assembly which the local and transient dehybridization of DNA hydrogel would lower the energy barrier for particle assembly under a magnetic field and then re-gelate to fix the pattern. This can be erased at a later time by de-hybridization in the absence of a magnetic field. e) Schematic of sample preparation and imaging. f) Digital photographs (state i-vi) of the same hydrogel sample at different conditions showing color changes, scale bar 600 μm. g) Reflectance spectra that correspond to the photographs in f), displaying the emerging reflectance peak ~530 nm after the in-situ assembly, which corresponds to the Bragg diffraction of in-situ assembled PC.

Results and discussion

As a proof-of-concept, we tested our design using bulk heating to drive DNA denaturation. After mixing the MNP solution with the palindromic ssDNA, we heated the sample to 90 °C in potassium phosphate buffer (37 mM, pH = 7) to form a homogeneous solution. The solution was cast on a preheated glass surface and then sandwiched using a second glass slide (**Figure 1e**). A thin film of the mixture was then allowed to cool to room temperature, thus forming a hydrogel (**Figure 1f**). The formed gel displayed a brown color, and its reflection spectra lacked any clear features (state i in **Figure 1f** and **1g**).

Neither the physical appearance of the material nor its reflection spectra changed when a magnetic field (~200 Gauss) was applied to the gel (state ii in **Figure 1f** and **1g**). Likewise no change was observed when the gel was only heated (90 °C) (state iii in **Figure 1f** and **1g**). However, when the gel was heated (90 °C) while simultaneously applying a magnetic field (~200 Gauss), green coloration appeared that was consistent with the appearance of a reflection band λ = 530 nm, thus confirming formation of the PC (state iv in **Figure 1f** and **1g**). The PC was maintained even after cooling the sample to room temperature (state v in **Figure 1f** and **1g**). Notably, heating the sample without applying an external magnetic field disrupted the structural color and allowed the material to return to its original non-PC (brown color) state (state vi in **Figure 1f** and **1g**). These results support the model described in **Figure 1d** and suggest the feasibility of reversible patterning of the PC with a photothermal input.

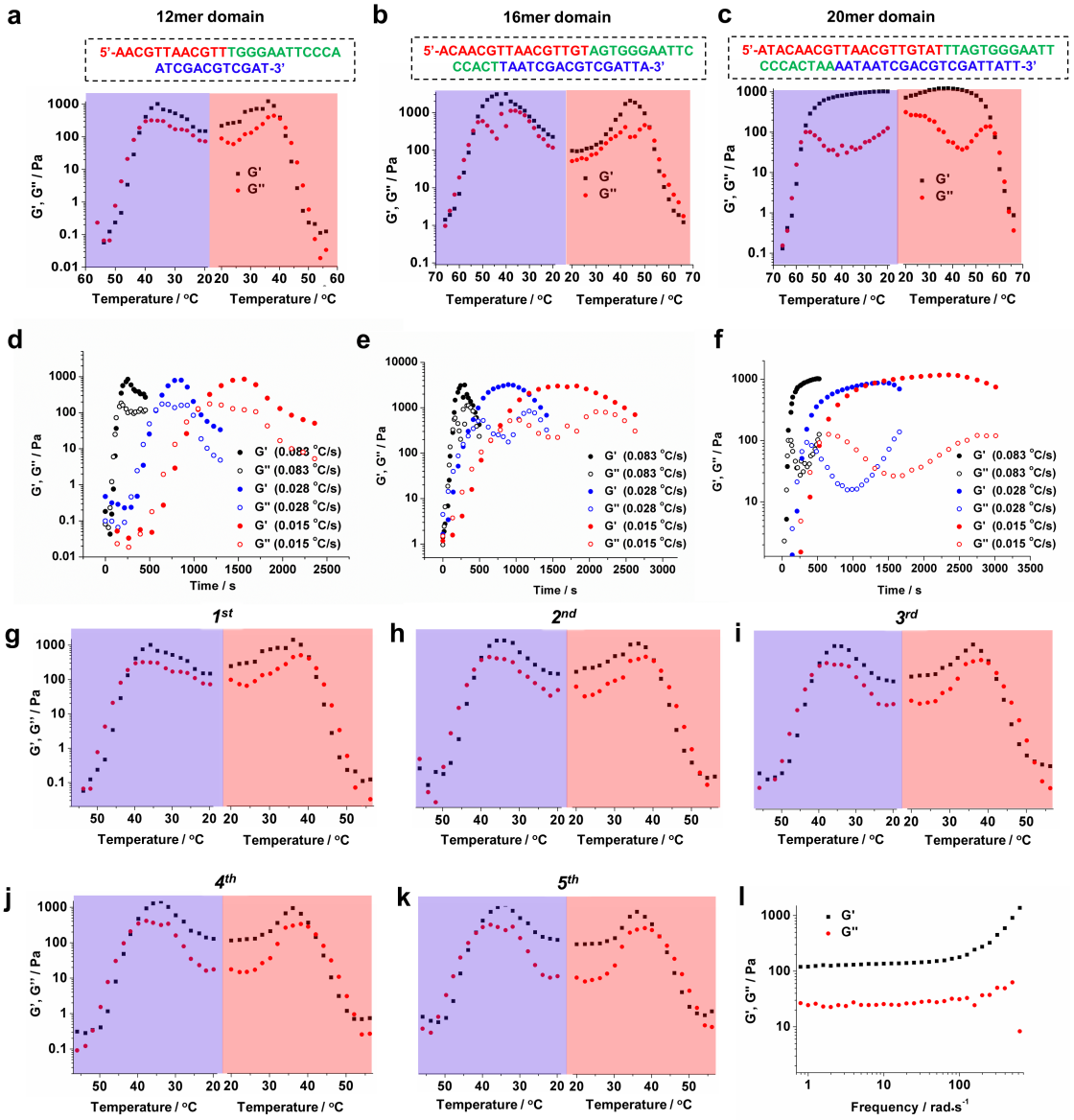

Figure 2. Rheology characterization of DNA supramolecular hydrogel/MNP composites. a-c) Rheology plots during cooling-heating cycles of PC hydrogels. The DNA supramolecular hydrogel is designed with three different sequences with palindromic domain lengths of 12,16, and 20 bases corresponding to a), b), and c), respectively. d-f) Rheology results using different scan rates (0.083, 0.028, and 0.015 °C/s) for different PC hydrogels shown in a-c). g-k) The cooling-heating cycles of PC hydrogels formation from 12mer palindromic domain DNA sequence. l) A frequency scan at room temperature of PC hydrogel formation with 12mer domain DNA strands to test the integrity of the hydrogel (G'>G'').

To better understand the gelation behavior of the DNA photonic hydrogel, we next performed rheology measurements as a function of DNA sequence, gelation time, and temperature. Firstly, three different sequences were designed and used to create DNA/nanoparticle composite hydrogels. Each sequence contained three palindromic domains of increasing length, 12, 16, and 20 oligomers (**Fig. 2a-c**). **Figure 2a-c** shows that gelation was reversible within just a single cooling (purple) and heating (red) cycle. At elevated temperatures, all samples were in a low-viscosity liquid state as G' was similar to G'' and their values were fairly low. As the temperature dropped, DNA hybridization proceeds, and this leads to gelation of the material as indicated with a drastic increase in G' and G'' and G'>G''. The apparent peak in G' and G'' is likely due to the volume change in the hydrogel due to hybridization[34]. We have also synthesized two additional sizes of MNPs to test the influence of particle size on the rheology of the hydrogel. We did not find a significant difference in rheology for DNA hydrogels embedded with 140, 180, and 200 nm diameter MNPs (**Figure S5**).

To investigate the effect of DNA sequence on gelation kinetics, we performed time-dependent rheology measurements. In principle, longer sequences should display slower hybridization kinetics and hence longer gelation times. Surprisingly, rheology measurements showed nearly identical gelation kinetics for the three sequences (**Figure 2d-f**). This is likely because the gelation time of the DNA is rapid and proceeds at time scales exceeding the time resolution of the rheometer (~0.083 ^{o}C/s). Thus, this indicate the palindromic DNA gelation

kinetics are fast, which is advantageous to achieve our goal of on-demand formation of PC structure *vide infra*.

In order to test the reversible gelation behavior, we additionally performed rheology measurements while running multiple thermal cycles on the DNA composite hydrogel formed by the 12-mer domain (**Figure 2g-k**). We found that the gelation behavior does not significantly change even after 5 heating-cooling cycles and the sample showed classic hydrogel behavior (G'>G'') at room temperature following thermal cycling. These results confirm the possibility of generating erasable PC patterns by repeated thermal cycling of the DNA hydrogels.

Figure 2l shows a plot of the G' and G'' as a function of frequency at room temperature. The data confirms that G'> G'' across the tested frequencies showing classic hydrogel behavior. We were unable to plot G' and G'' above the transition temperature, as the gel was completely liquid and displayed the minimum G' and G'' reportable values of ~0.02 Pa which is the limit of the rheometer resolution. These palindromic DNA hydrogels are rheologically distinct from hybrid gels comprised of acrylamide polymers crosslinked using DNA. The rheology measurements for the acrylamide-DNA gels showed a relatively high G' above the transition temperature, which is likely due to the entanglement of its long polymer backbone (**Figure S6**). Therefore, acrylamide-DNA gels would still significantly hinder the reorganization of MNPs above the transition temperature so that on-demand assembly of PC would fail (**Figure**

S7). Hence, this particular 3-domain palindromic DNA offers properties that are advantageous for the goal of on-demand assembly of PC structures.

To provide further evidence of light and magnetic field driven assembly of the MNPs into a PC structure within the DNA hydrogel, we employed high-resolution optical microscopy to observe the microscopic assembly of the particles. In our microscope setup, we observed the MNPs by using reflection interference contrast microscopy (RICM) at λ_{ex} = 535 nm while simultaneously exciting the region of interest using a galvo-controlled ~5 μm diameter 785 nm laser irradiation system (**Figure 3a**). We used a rare earth magnet to generate a magnetic field (~100 Gauss) that drives the assembly of MNPs in a direction that is parallel to the magnetic field and the observation plane. **Figure 3b** shows RICM images displaying the organization of the MNPs prior to and after near-IR illumination (785 nm) for 10 sec (red circle; duty cycle 50%; power = 36.2 mW; on-time = 500 msec). We note the formation of linear assemblies of particles that align with the external magnetic field. To demonstrate the reversibility of PC assembly, we next illuminated the same region for another 10 sec (red circle; duty cycle 50%; power =36.2 mW; on-time = 500 msec) in the absence of the magnetic field. The bottom two images in **Figure 3b** show the loss of particle organization in the absence of the external magnetic field. Importantly, particle assembly was confined to the near-IR illumination area while the remaining regions showed static particles that remained randomly distributed (**Supplementary Video 1** and **2**, also see **Video 3** and **4** for patterning with different direction of magnetic field on a single piece of hydrogel). Similar results were also found in DNA

hydrogels with the 140 and 200 nm diameter MNPs (**Figure S8**). We also performed z-stack scanning in the RICM channel and generated 3D reconstruction images (in ImageJ) to further identify the linear assemblies of MNPs inside the gel after alignment where the MNPs assemblies are erased (**Figure 3c**). Quantitative analyses of alignment were conducted using the ridge detection plugin[35] of ImageJ (**Figure S9**), which allowed us to measure an in-plane Feret angle for the linear assemblies using the microscope image frame of reference where θ=0°, which is parallel to the *x*-axis and serves as the frame of reference. **Figure 3d** and **e** show radial histograms and box plots, respectively, that were collected from three regions of interest after alignment and erasing of the linear assemblies as described above. In figure 3d, the fan area indicates the angle distribution. The largest area from Feret angle of the aligned MNPs was the area that represents 0-30°, coinciding with the approximate direction of the magnetic field (as illustrated in **Figure 3b**). After erasing, the angle preference was lost since other fan areas grow nearly as large as the one that represents 0-30°. In box plots (**Figure 3e**), the data points of the original sample showed a uniform distribution span from 0 to 180°. However, most of the data points converge to ~30° after alignment, which indicates an angle of interest that is similar to **Figure 3d**. This alignment is lost again in the box plot that represent the erased sample. To summarize, the laser and magnetic field induced on-demand patterning is effective and swift as expected.

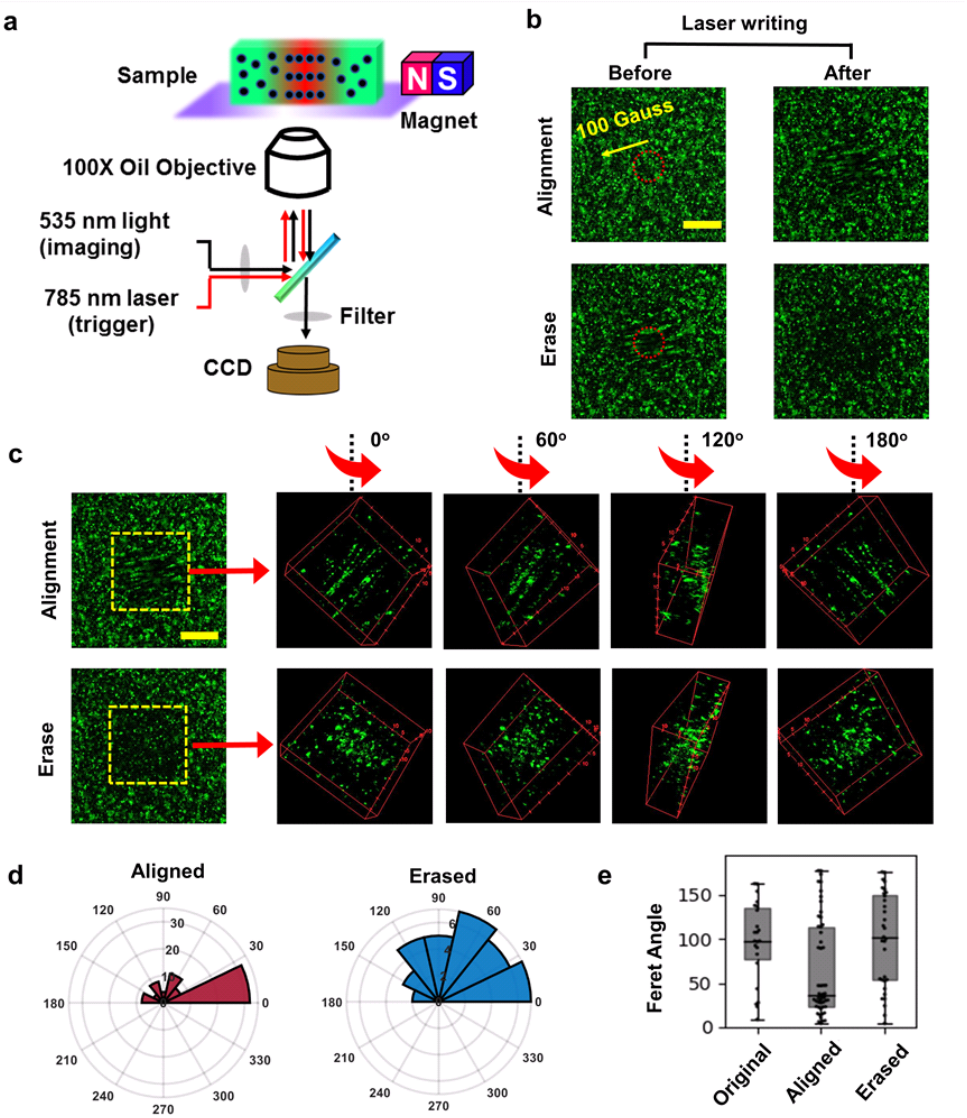

Figure 3. Microscopic imaging results of on-demand assembly. a) Schematic of microscope settings for in-situ imaging. The sample was on a glass slide and observed by 100X oil objective with an optical path to a CCD camera and 785 nm laser controlled by a galvo-mirror system for spatially selective excitation. b) Comparison of nano-pattern changes inside the hydrogel before and after applying laser irradiation. Upper set: laser writing of PC nano-patterns. Lower set: laser erasing of PC nano-patterns. (Scale bar: 20 μm) c) 3D reconstructed images based on z-scans of the sample at different angles of rotation demonstrating organized or disorganized structures inside the hydrogel. (Scale bar: 20 μm) d) Feret angles plotted in histogram based on statistical analysis of aligned or erased structures that correspond to automated object detection ridge analysis of sample images. e) Box plot shows the statistical analysis of Feret angles measured from original, aligned or erased samples.

On-demand and in-situ assembly of PC structure in hydrogels has many potential applications. One of these applications is for on-demand writing/erasing which was described recently[36-38]. To demonstrate this potential application using our approach, we conducted a series of writing/erasing tests in the DNA hydrogel samples. As described above, photo-thermal heating can trigger local melting of the DNA, thus minimizing the energy barrier of MNP translocation and allowing for on-demand assembly. Our first goal was to quantify how the irradiation time and power tune the local assembly and coloration of the PC gel. Hence we designed an array of irradiation spots with different laser powers (40%–100%) and irradiation times (1–5 sec), and captured images of the gel before and after illumination (**Figure 4a**). The experiment was conducted under an external magnetic field that was perpendicular to the observation plane. We found that the color of the PC gel did not change when the total input energy was low; either when the illumination time was brief or if the illumination intensity was weak (e.g. 40% laser power, 1s irradiation time). At greater illumination intensities and dwell times, we observed the diameter of the spots increased as a function of the energy input (**Figure 4b**). This is likely due to the accumulation of heat allowing for melting of greater regions of DNA and migration of greater numbers of MNPs from the surrounding hydrogel. We also observed formation of spots that seemed to have a colored ring and dark center. According to our investigation, the dark center is likely due to the depletion of DNA because the hydrogel unevenly re-distributed after heating/cooling (**Figure S10**). This is supported by control experiments using fluorophore labeled ssDNA (**Figure S11**). We found that a laser power of 80% with 3 s irradiation time produced optimal results since the spot size produced

sufficient contrast from the background and the spot size was smaller suggesting improvement in spatial resolution. We also find that the spot size is related to particle concentration. The melting area changed drastically when we photothermally heated the hydrogel sample. This is due to the higher particle concentration for the samples with greater wt% which produces greater amounts of heat upon illumination **(Figure S12).** By applying this protocol using patterns with pre-assigned (x,y) coordinates, we first created a 3-leaf clover-like figure with an area of 1-2 mm^2 which was spatially patterned and erased after bulk heating and cooling (**Figure 4c,** also see **Supplementary video 5**). We also demonstrated the patterning of a QR code (2 mm x 2 mm) encrypting with text information of "Emory 1836" in **Figure 4d**. Information can be stored and later read using a smart device (**Supplementary video 6**) as we showed in this figure. In our system, this pattern comprised of ~250 spots required approximately 10 min to complete with a single laser illumination system, thus demonstrating the ability to create patterns on-demand. Compared to rewritable technology based on photochromic materials[39], our method is free of photobleaching, does not require a photomask, and generates patterns more rapidly.

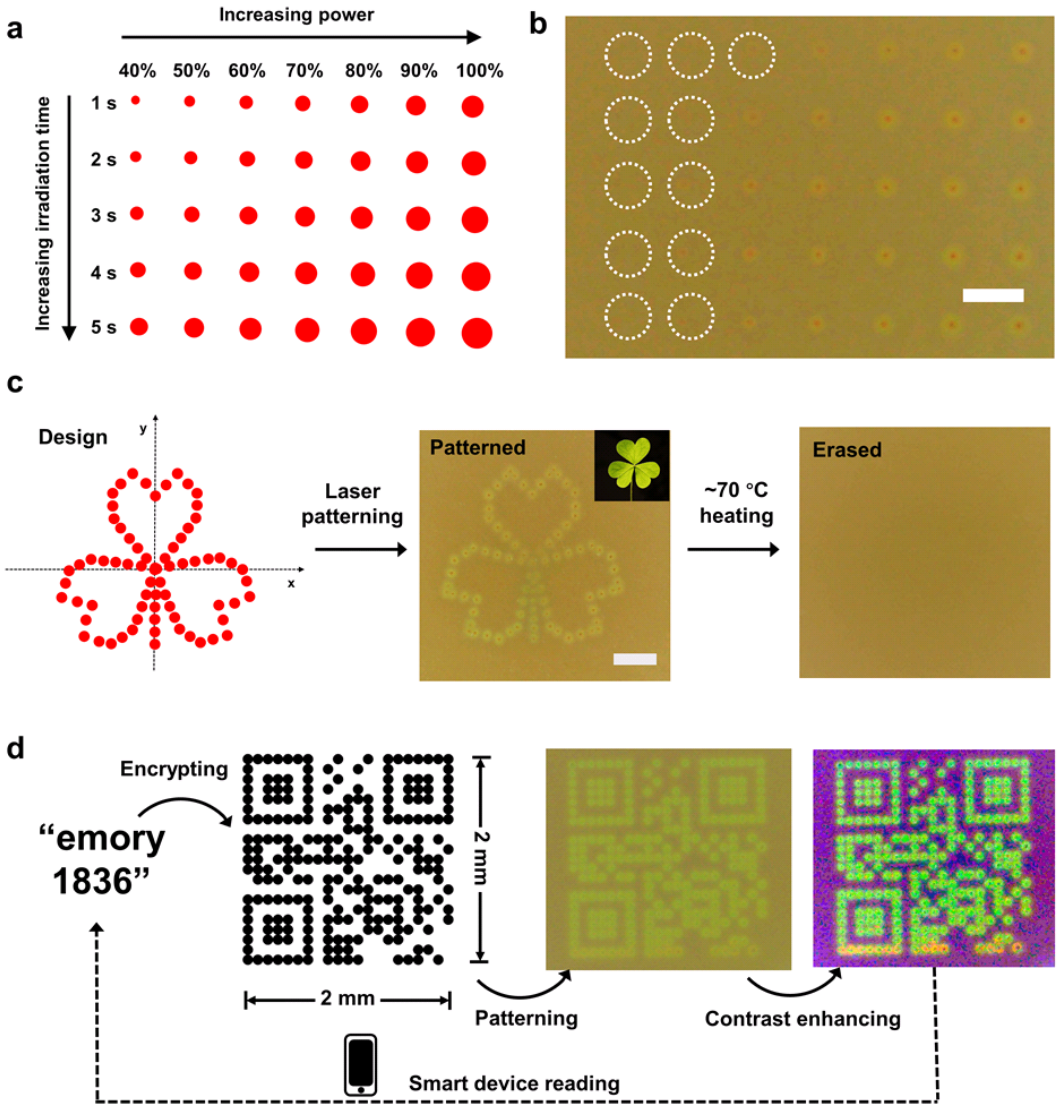

Figure 4. Laser patterning demonstrations of in-situ assembly of DNA supramolecular hydrogels. a) Laser patterning map based on different laser power and laser irradiation times. Note that 100% laser power is around 49.7 mW. b) Digital photograph of the laser patterned spots based on the design of a) (scale bar 300 μm). c) A laser patterning design of a 3-leaf clover after the patterning and the real image (top inset). The patterned image can be erased by bulk heating. Scale Bar 400 μm. d) A flow diagram demonstrates encrypting application of on-demand assembly. A QR code encrypting the text "emory 1836" was generated first by software. Then, we photo-patterned the QR code (2 mm x 2 mm) with on-demand assembly technology in this work. After adjusting the contrasts of the microscope image, the QR code was read by a smart device to reveal the encrypted information. Note: All hydrogels were imaged at room temperature in the absence of a magnetic field.

Conclusion

In summary, we demonstrate an on-demand structural color patterning technology using a DNA supramolecular hydrogel system with high spatial and temporal resolution. The gel is crosslinked using all non-covalent Watson-Crick-Franklin interactions which are advantageous because these can be easily programmed. The self-assembly of MNP created PC structural color which could be controlled and erased on demand based on specific thermal, optical and magnetic inputs. Rheology measurements of the hydrogel composite show highly reversible and rapid crosslinking/de-crosslinking kinetics which were observed for the three palindromic DNA sequences tested (12, 16, and 20 mer domains). Generating PC coloration required transient de-crosslinking of the gel while simultaneously applying an external magnetic field to assemble the MNP. This coloration was rapidly erased when the gels were transiently de-crosslinked in the absence of a magnetic field. Because of the strong visible and near-IR absorbance of the MNPs, structural color could be patterned in a facile manner using a near-IR laser source with micrometer spatial resolution and sub-sec temporal resolution. It is important to note that there are many reported examples of re-writable materials and these are based on photochromic (REF), PC (REF) and metal-organic framework (MOF) (REF) materials. In contrast to photochromic materials, PCs offer more stable coloration that resists photobleaching and degradation that is well documented for organic dyes and pigments. Other PC-rewritable approaches display slow response times (for writing and erasing) as these

systems require a volumetric swelling/deswelling change in the polymer matrix. For example, Chen et al. report of reversible PC coloration required ~10 min response times (REF). By leveraging the rapid and highly localized gelation/de-gelation kinetics of palindromic DNA our strategy offers high spatial resolution (up to ~10 μm), direct-write color patterning without the need for a photomask, and with rapid patterning (<1s) and erasing time (<10s). Supplementary information Table 1 compares some of the reported technologies to generate re-writable materials. Finally, we note that the fundamental strategy disclosed here might inspire other applications such as chemical sensing, molecular diagnostics, and information storage due to the programmability and sensitivity of DNA-based hydrogels.

ASSOCIATED CONTENT

The Supporting Information is listed below

Experimental section, Characterization, Reflection spectra of nanoparticle assembly, TEM images with different sizes of MNPs, Proof of concept experiment for photo-thermal dehybridization, Finite element simulation of photothermal effect of MNPs, Rheology test for DNA duplex crosslinked polyacrylamide hydrogel, Microscope images of attempted particle re-alignment in synthetic polymer hydrogel crosslinked by DNA duplex, Examples of ridge detection, Fluorescence microscope images (.PDF)

Supplementary video 1 (.avi)

Supplementary video 2 (.avi)

Supplementary video 3 (.avi)

Supplementary video 4 (.avi)

Supplementary video 5 (.avi)

Supplementary video 6 (.mp4)

AUTHOR INFORMATION

***Corresponding author:**

Khalid Salaita - Department of Chemistry, Emory University, 1515 Dickey Drive, Atlanta, Georgia, 30322, USA; Email: k.salaita@emory.edu

Authors:

Yixiao Dong - Department of Chemistry, Emory University, 1515 Dickey Drive, Atlanta, Georgia, 30322, USA

J. Dale Combs - Department of Chemistry, Emory University, 1515 Dickey Drive, Atlanta, Georgia, 30322, USA

Cong Cao - Department of Physics, Emory University, 400 Dowman Drive Atlanta, Georgia, 30322, USA

Eric R. Weeks - Department of Physics, Emory University, 400 Dowman Drive Atlanta, Georgia, 30322, USA

Alisina Bazrafshan - Department of Chemistry, Emory University, 1515 Dickey Drive, Atlanta, Georgia, 30322, USA

SK Aysha Rashid - Department of Chemistry, Emory University, 1515 Dickey Drive, Atlanta, Georgia, 30322, USA

Author Contributions

Y.D. and K.S. conceived of the project. Y.D. designed and performed most of the experiments. J.D.C helped with the in-situ imaging, statistical analysis, and related discussions. C.C. and E. R. W. helped with rheological experiments and related discussions. A.B. helped with proof of concept experiments. SK A. R. helped with laser patterning demonstration. K.S and Y.D. wrote the manuscript. All the authors helped revise the manuscript.

Notes

The authors declare no conflict of interest.

ACKNOWLEDGMENT

This work is supported by NIH R01 GM 131099, and NIH R01 GM 124472. The authors especially thank Dr. Yonggang Ke from the department of biomedical engineering at Emory University for his 3-domain ssDNA design.

REFERENCES

1. Zhao, Z.; Fang, R.; Rong, Q.; Liu, M., Bioinspired nanocomposite hydrogels with highly ordered structures. *Adv. Mater.* **2017,** *29* (45), 1703045.

2. Mao, L.-B.; Gao, H.-L.; Yao, H.-B.; Liu, L.; Cölfen, H.; Liu, G.; Chen, S.-M.; Li, S.-K.; Yan, Y.-X.; Liu, Y.-Y., Synthetic nacre by predesigned matrix-directed mineralization. *Science* **2016,** *354* (6308), 107-110.

3. Sano, K.; Arazoe, Y. O.; Ishida, Y.; Ebina, Y.; Osada, M.; Sasaki, T.; Hikima, T.; Aida, T., Extra-Large Mechanical Anisotropy of a Hydrogel with Maximized Electrostatic Repulsion between Cofacially Aligned 2D Electrolytes. *Angew. Chem. Int. Ed.* **2018,** *57* (38), 12508-12513.

4. Hua, M.; Wu, S.; Ma, Y.; Zhao, Y.; Chen, Z.; Frenkel, I.; Strzalka, J.; Zhou, H.; Zhu, X.; He, X., Strong tough hydrogels via the synergy of freeze-casting and salting out. *Nature* **2021,** *590* (7847), 594-599.

5. Dong, Y.; Bazrafshan, A.; Pokutta, A.; Sulejmani, F.; Sun, W.; Combs, J. D.; Clarke, K. C.; Salaita, K., Chameleon-inspired strain-accommodating smart skin. *ACS Nano* **2019,** *13* (9), 9918-9926.

6. Hu, Z.; Sun, H.; Thompson, M. P.; Xiao, M.; Allen, M. C.; Zhou, X.; Ni, Q. Z.; Wang, Z.; Li, W.; Burkart, M. D.; Deheyn, D. D.; Dhinojwala, A.; Shawkey, M. D.; Gianneschi, N. C., Structurally Colored Inks from Synthetic Melanin-Based Crosslinked Supraparticles. *ACS Materials Letters* **2021,** *3* (1), 50-55.

7. Yang, X.; Qiu, L.; Cheng, C.; Wu, Y.; Ma, Z. F.; Li, D., Ordered gelation of chemically converted graphene for next-generation electroconductive hydrogel films. *Angew. Chem. Int. Ed.* **2011,** *50* (32), 7325-7328.

8. Wong, T.-S.; Kang, S. H.; Tang, S. K.; Smythe, E. J.; Hatton, B. D.; Grinthal, A.; Aizenberg, J., Bioinspired self-repairing slippery surfaces with pressure-stable omniphobicity. *Nature* **2011,** *477* (7365), 443-447.

9. Yao, X.; Wang, J.; Jiao, D.; Huang, Z.; Mhirsi, O.; Lossada, F.; Chen, L.; Haehnle, B.; Kuehne, A. J. C.; Ma, X.; Tian, H.; Walther, A., Room-Temperature Phosphorescence Enabled through Nacre-Mimetic Nanocomposite Design. *Adv. Mater.* **2021,** *33* (5), 2005973.

10. Lossada, F.; Abbasoglu, T.; Jiao, D.; Hoenders, D.; Walther, A., Glass Transition Temperature Regulates Mechanical Performance in Nacre-Mimetic Nanocomposites. *Macromol. Rapid Commun.* **2020,** *41* (20), 2000380.

11. Kim, Y. S.; Liu, M.; Ishida, Y.; Ebina, Y.; Osada, M.; Sasaki, T.; Hikima, T.; Takata, M.; Aida, T., Thermoresponsive actuation enabled by permittivity switching in an electrostatically anisotropic hydrogel. *Nat. Mater.* **2015,** *14* (10), 1002-1007.

12. Sidorenko, A.; Krupenkin, T.; Taylor, A.; Fratzl, P.; Aizenberg, J., Reversible Switching of Hydrogel-Actuated Nanostructures into Complex Micropatterns. *Science* **2007,** *315* (5811), 487-490.

13. Khodambashi, R.; Alsaid, Y.; Rico, R.; Marvi, H.; Peet, M. M.; Fisher, R. E.; Berman, S.; He, X.; Aukes, D. M., Heterogeneous hydrogel structures with spatiotemporal reconfigurability using addressable and tunable voxels. *Adv. Mater.* **2021,** *33* (10), 2005906.

14. Alapan, Y.; Karacakol, A. C.; Guzelhan, S. N.; Isik, I.; Sitti, M., Reprogrammable shape morphing of magnetic soft machines. *Science advances* **2020,** *6* (38), eabc6414.

15. Zhang, J.; Guo, Y.; Hu, W.; Soon, R. H.; Davidson, Z. S.; Sitti, M., Liquid Crystal Elastomer-Based Magnetic Composite Films for Reconfigurable Shape-Morphing Soft Miniature Machines. *Adv. Mater.* **2021,** *33* (8), 2006191.

16. Cui, J.; Huang, T.-Y.; Luo, Z.; Testa, P.; Gu, H.; Chen, X.-Z.; Nelson, B. J.; Heyderman, L. J., Nanomagnetic encoding of shape-morphing micromachines. *Nature* **2019,** *575* (7781), 164-168.

17. Yue, Y.; Kurokawa, T.; Haque, M. A.; Nakajima, T.; Nonoyama, T.; Li, X.; Kajiwara, I.; Gong, J. P., Mechano-actuated ultrafast full-colour switching in layered photonic hydrogels. *Nat. Commun.* **2014,** *5* (1), 1-8.

18. Zhang, S.; Greenfield, M. A.; Mata, A.; Palmer, L. C.; Bitton, R.; Mantei, J. R.; Aparicio, C.; De La Cruz, M. O.; Stupp, S. I., A self-assembly pathway to aligned monodomain gels. *Nat. Mater.* **2010,** *9* (7), 594-601.

19. Zhang, J.-T.; Wang, L.; Luo, J.; Tikhonov, A.; Kornienko, N.; Asher, S. A., 2-D array photonic crystal sensing motif. *J. Am. Chem. Soc.* **2011,** *133* (24), 9152-9155.

20. Chen, Q.; Wang, C.; Wang, S.; Zhou, J.; Wu, Z., A responsive photonic crystal film sensor for the ultrasensitive detection of uranyl ions. *Analyst* **2020,** *145* (16), 5624-5630.

21. Cai, Z.; Sasmal, A.; Liu, X.; Asher, S. A., Responsive photonic crystal carbohydrate hydrogel sensor materials for selective and sensitive lectin protein detection. *ACS sensors* **2017,** *2* (10), 1474-1481.

22. Chen, K.; Zhang, Y.; Ge, J., Highly invisible photonic crystal patterns encrypted in an inverse opaline macroporous polyurethane film for anti-counterfeiting applications. *ACS Appl. Mater. Interfaces* **2019,** *11* (48), 45256-45264.

23. Lee, G. H.; Choi, T. M.; Kim, B.; Han, S. H.; Lee, J. M.; Kim, S.-H., Chameleon-inspired mechanochromic photonic films composed of non-close-packed colloidal arrays. *ACS Nano* **2017,** *11* (11), 11350-11357.

24. Yang, Y.; Chen, Y.; Hou, Z.; Li, F.; Xu, M.; Liu, Y.; Tian, D.; Zhang, L.; Xu, J.; Zhu, J., Responsive Photonic Crystal Microcapsules of Block Copolymers with Enhanced Monochromaticity. *ACS Nano* **2020,** *14* (11), 16057-16064.

25. Yue, Y.; Kurokawa, T., Designing responsive photonic crystal patterns by using laser engraving. *ACS Appl. Mater. Interfaces* **2019,** *11* (11), 10841-10847.

26. Jia, X.; Xiao, T.; Hou, Z.; Xiao, L.; Qi, Y.; Hou, Z.; Zhu, J., Chemically Responsive Photonic Crystal Hydrogels for Selective and Visual Sensing of Thiol-Containing Biomolecules. *ACS omega* **2019,** *4* (7), 12043-12048.

27. Yang, B.; Li, L.; Du, K.; Fan, B.; Long, Y.; Song, K., Photo-responsive photonic crystals for broad wavelength shifts. *Chem. Commun.* **2018,** *54* (24), 3057-3060.

28. Goodling, A. E.; Nagelberg, S.; Kolle, M.; Zarzar, L. D., Tunable and responsive structural color from polymeric microstructured surfaces enabled by interference of totally internally reflected light. *ACS Materials Letters* **2020,** *2* (7), 754-763.

29. Ge, J.; Yin, Y., Responsive photonic crystals. *Angew. Chem. Int. Ed.* **2011,** *50* (7), 1492-1522.

30. Nucara, L.; Greco, F.; Mattoli, V., Electrically responsive photonic crystals: a review. *J. Mater. Chem. C* **2015,** *3* (33), 8449-8467.

31. Hansing, J.; Netz, R. R., Hydrodynamic Effects on Particle Diffusion in Polymeric Hydrogels with Steric and Electrostatic Particle–Gel Interactions. *Macromolecules* **2018,** *51* (19), 7608-7620.

32. Parrish, E.; Caporizzo, M. A.; Composto, R. J., Network confinement and heterogeneity slows nanoparticle diffusion in polymer gels. *The Journal of Chemical Physics* **2017,** *146* (20), 203318.

33. Jiang, H.; Pan, V.; Vivek, S.; Weeks, E. R.; Ke, Y., Programmable DNA hydrogels assembled from multidomain DNA strands. *Chembiochem* **2016,** *17* (12), 1156-1162.

34. Topuz, F.; Okay, O., Rheological behavior of responsive DNA hydrogels. *Macromolecules* **2008,** *41* (22), 8847-8854.

35. Steger, C., An unbiased detector of curvilinear structures. *IEEE Transactions on pattern analysis and machine intelligence* **1998,** *20* (2), 113-125.

36. Chen, C.; Zhao, X.; Chen, Y.; Wang, X.; Chen, Z.; Li, H.; Wang, K.; Zheng, X.; Liu, H., Reversible Writing/Re-Writing Polymeric Paper in Multiple Environments. *Adv. Funct. Mater.* **2021**, 2104784.

37. Chen, L.; Weng, M.; Huang, F.; Zhang, W., Long-lasting and easy-to-use rewritable paper fabricated by printing technology. *ACS Appl. Mater. Interfaces* **2018,** *10* (46), 40149-40155.

38. Müller, V.; Hungerland, T.; Baljozovic, M.; Jung, T.; Spencer, N. D.; Eghlidi, H.; Payamyar, P.; Schlüter, A. D., Ink-Free Reversible Optical Writing in Monolayers by Polymerization of a Trifunctional Monomer: Toward Rewritable "Molecular Paper". *Adv. Mater.* **2017,** *29* (27), 1701220.

39. Khazi, M. I., Jeong, W., & Kim, J. M. Functional materials and systems for rewritable paper. *Adv. Mater.* **2018**, *30* (15), 1705310.